DALTON
FULL PAPER

Tuning the metal–metal separation in pyrazolate-based dinuclear complexes by the length of chelating side arms‡

Franc Meyer,*† Katja Heinze, Bernhard Nuber and Laszlo Zsolnai

Anorganisch-Chemisches Institut der Universität Heidelberg, Im Neuenheimer Feld 270, D-69120 Heidelberg, Germany

Six dinuclear cobalt(II) complexes of pyrazolate ligands with multidentate chelating side arms {3,5-$(R_2NCH_2)_2C_3N_2H_2$; R_2N = $[Me_2N(CH_2)_3]_2N$ (HL^1) or $(Et_2NCH_2CH_2)_2N$ (HL^2)} have been prepared and characterised. The reaction of L^1 and L^2 with 2 equivalents of $[Co(MeCN)_6][BF_4]_2$ and $NaBPh_4$ proceeds *via* the isolable compounds $[Co_2L^1(BF_4)][BPh_4]_2$ **1a** and $[Co_2L^2(BF_4)][BPh_4]_2$ **2a** finally to afford the dinuclear complexes $[Co_2L^1F][BPh_4]_2$ **1b** and $[Co_2L^2(F)(H_2O)][BPh_4]_2$ **2b**, respectively, where a fluoride has been abstracted from the BF_4^- starting material in both cases. While the longer side arms in **1b** allow for an exogenous bridging position of the fluoride, an additional water molecule is incorporated in **2b** to form an FHO(H) moiety with an unusually short F–H–O bridge between the two cobalt centres. Evidence is reported for the reversible extrusion of the water molecule from **2b**. Treatment of **2b** with KBr or NaN_3 yielded the respective bromide- and azide-bridged complexes **3** and **4**, where in the latter case the azide adopts a μ-1,3-bridging mode. The magnetic properties of **3** and **4** have been studied in the temperature range 8–200 K. Complexes **1b**, **2b**, **3** and **4** were also characterised by means of X-ray crystallography.

Stimulated by the occurrence of bi- and multi-metallic centres in the active sites of various metalloenzymes, there is considerable current interest in transition-metal complexes containing several metal ions in close proximity.[1] In order to control possible co-operative phenomena between the two metal centres the design of appropriate ligand cores providing co-ordination sites with well defined metal–metal separations is highly desirable.[2] Many of the dinucleating ligand systems reported are derived from bridging phenoxide or alkoxide moieties containing additional chelating donors, in which a single oxygen centre spans the two metal ions in a dinuclear arrangement.[3] These monoatomic bridges generally support metal–metal separations in the range 2.5–3.8 Å. Larger separations are accessible by using diatomic bridges and should be adjustable by means of additional chelating side arms connected with the bridging framework. The ability of the 1,2-diazole unit of pyrazolates to bridge two metal ions is well documented.[4] However, relatively few studies of dinuclear complexes of pyrazolate-based ligands possessing additional chelating substituents in the 3 and 5 positions of the heterocycle have been reported until now.[5–9] Recently we reported a series of dinuclear cobalt(II) complexes **A** of pyrazolate ligands providing multidentate nitrogen donors within side arms of varying chain lengths.[9a] Force-field calculations showed that the two tran-type co-ordination subunits [tran = tris(aminoalkyl)-amine] of these bimetallic systems are largely decoupled with respect to their accessible conformational space, which should allow the adaptation to different secondary bridges X. However, those complexes studied previously all contain chloride ions as secondary bridging ligands,[9a] which thus determined the effective Co···Co distances and caused the latter to be very similar irrespective of the chain lengths of the substituents at the pyrazolate. Based on the same basic structural motif the present work describes the adjustment of different metal–metal separations and hence the preference for matching secondary anions X in this type of system, induced by the different lengths of the donor side arms.

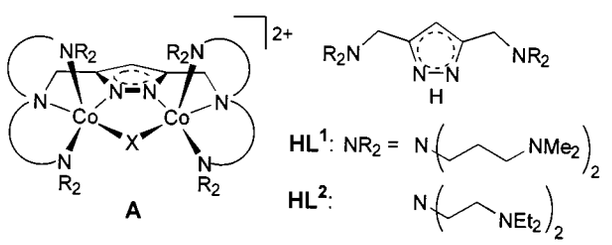

Results and Discussion

In an attempt to introduce a weakly co-ordinating anion as the secondary bridge X in complexes of type **A**, the deprotonated pyrazolate derivative L^1 was treated with 2 equivalents of $[Co(MeCN)_6][BF_4]_2$ in acetonitrile, immediately yielding a deep purple solution. Anion exchange with 2 equivalents of $NaBPh_4$ and subsequent addition of diethyl ether caused precipitation of a purple solid, which after its isolation gave analytical data in accord with the sought composition $[Co_2L^1(BF_4)][BPh_4]_2$ **1a**. Attempts to crystallise **1a** by vapour diffusion of diethyl ether into an acetonitrile solution over a period of several days resulted in the formation of purple crystals, which however gave rise to IR and analytical data different from those of the initially formed complex **1a**, in particular not showing any IR absorption typical for BF_4^- ions. The X-ray crystal analysis of the new complex **1b**, the structure of which is given in Fig. 1, revealed that a fluoride ion was abstracted from the BF_4^- and incorporated in the bridging position between the two cobalt atoms. Ample precedent is indeed reported for such a process, as fluorinated counter ions of the type BF_4^- or PF_6^- have long been known to be potentially reactive sources of fluoride.[10,11]

The molecular structure of the cation of complex **1b** shows a μ-pyrazolato-μ-fluoro-dicobalt(II) core with the co-ordination geometry around each cobalt centre being intermediate between distorted trigonal bipyramidal [the bridging fluoride and the branching nitrogen N(3) and N(6) in axial positions] and distorted square pyramidal [N(5) and N(8) occupying the apical positions]. The central atoms Co(1), F, Co(2), N(2) and N(1) form a cyclic array (planar within 0.013 Å) that is nearly coplanar with the plane of the pyrazolate heterocycle (intersect-

† E-Mail: franc@sun0.urz.uni-heidelberg.de

‡ *Non-SI units employed*: bar = 10^5 Pa, $\mu_B \approx 9.27 \times 10^{-24}$ J T^{-1}.

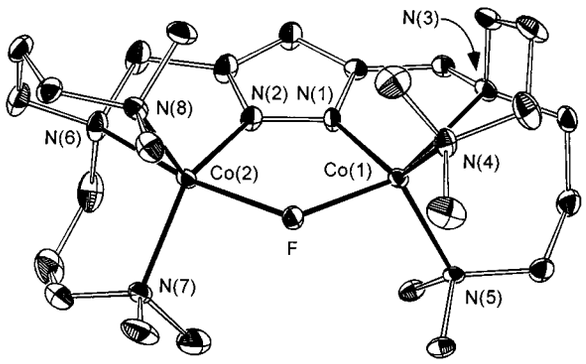

Fig. 1 View of the molecular structure of the cation of complex **1b** (30% probability ellipsoids). For clarity all hydrogen atoms have been omitted

Table 1 Selected atom distances (Å) and angles (°) for complex **1b**

Co(1)–N(1)	1.944(1)	Co(2)–N(6)	2.350(5)
Co(1)–N(3)	2.403(4)	Co(2)–N(7)	2.074(5)
Co(1)–N(4)	2.085(5)	Co(2)–N(8)	2.090(5)
Co(1)–N(5)	2.073(5)	Co(2)–F	2.077(3)
Co(1)–F	2.077(3)	N(1)–N(2)	1.365(6)
Co(2)–N(2)	1.945(4)	Co(1)···Co(2)	3.577
N(1)–Co(1)–N(3)	74.0(2)	N(2)–Co(2)–N(8)	114.0(2)
N(1)–Co(1)–N(4)	130.4(2)	N(2)–Co(2)–F	85.8(2)
N(1)–Co(1)–N(5)	111.5(2)	N(6)–Co(2)–N(7)	92.7(2)
N(1)–Co(1)–F	85.9(2)	N(6)–Co(2)–N(8)	90.4(2)
N(3)–Co(1)–N(4)	91.4(2)	N(6)–Co(2)–F	159.4(2)
N(3)–Co(1)–N(5)	89.1(2)	N(7)–Co(2)–N(8)	114.3(2)
N(3)–Co(1)–F	157.4(2)	N(7)–Co(2)–F	94.1(2)
N(4)–Co(1)–N(5)	115.4(2)	N(8)–Co(2)–F	104.3(2)
N(4)–Co(1)–F	93.9(2)	Co(1)–N(1)–N(2)	124.6(3)
N(5)–Co(1)–F	108.1(2)	Co(2)–N(2)–N(1)	124.8(3)
N(2)–Co(2)–N(6)	75.0(2)	Co(1)–F–Co(2)	118.9(2)
N(2)–Co(2)–N(7)	130.1(2)		

ing angle 2.9°). The structure of the cation of **1b** thus is very similar to those of the Cl-bridged analogue reported previously,[9a] however the smaller fluoride bridge results in a much shorter Co···Co separation of 3.577 Å (Table 1) in the present case as compared to 3.909 Å for the chloro-compound.

The readily occurring abstraction of fluoride from the original BF_4^- counter anion and its insertion between the two cobalt atoms in complex **1b** is probably enhanced by the strong tendency of pyrazolate-based dinuclear entities to incorporate additional secondary bridges. We thus assumed that the use of a primary dinucleating ligand with shorter chelating side arms, which can be shown from simple molecular models to pull the two metal centres further back and apart and create a bimetallic pocket not suited to fit a small anion like fluoride or hydroxide in a bridging fashion, might stabilise an intact BF_4^- counter anion in the bridging position. It should be noted in this context that we recently observed a F,F′-bridging BF_4^- ion in the solid state structure of a bis(μ-pyrazolato)-bridged dinuclear copper(II) complex.[9b]

Treatment of the deprotonated ligand L^2 with 2 equivalents of $[Co(MeCN)_6][BF_4]_2$ yields a purple solution, from which after anion exchange the light purple complex **2a** could be isolated. Its analytical data were in accord with the composition $[Co_2L^2(BF_4)][BPh_4]_2$, however all attempts to obtain single crystals of **2a** suitable for X-ray analysis unfortunately failed. When however a solution of **2a** in acetonitrile was treated with a small amount of water a spontaneous decolorisation took place and a pale grey complex formed. Single crystals of this compound **2b** were obtained by vapour diffusion of diethyl ether into an acetonitrile solution of the material. The IR spectrum of **2b** revealed broad bands at 3471 and 2612 cm^{-1} attributed to a hydrogen bridged OH group, and the overall structure of the complex was elucidated by a crystallographic study.

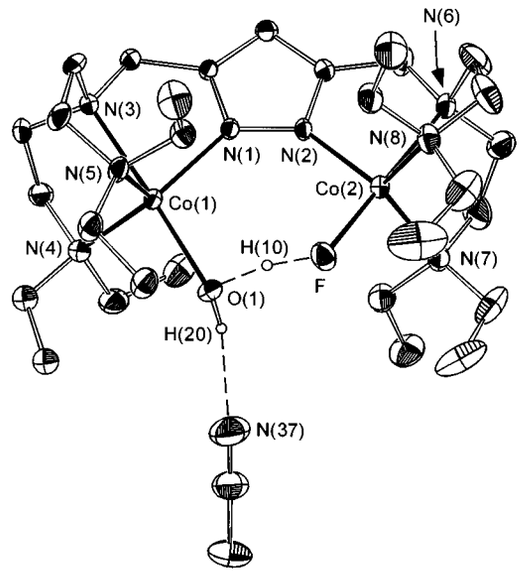

Fig. 2 View of the molecular structure of the cation of complex **2b**. Details as in Fig. 1

Table 2 Selected atom distances (Å) and angles (°) for complex **2b**

Co(1)–N(1)	2.042(4)	Co(2)–F	1.932(3)
Co(1)–N(3)	2.204(4)	N(1)–N(2)	1.378(5)
Co(1)–N(4)	2.141(5)	Co(1)···Co(2)	4.282
Co(1)–N(5)	2.157(4)	O(1)–H(10)	1.24(6)
Co(1)–O(1)	2.032(4)	O(1)–H(20)	0.80(3)
Co(2)–N(2)	2.040(4)	F–H(10)	1.23(6)
Co(2)–N(6)	2.201(4)	F···O(1)	2.437
Co(2)–N(7)	2.136(5)	O(1)···N(37)	2.957
Co(2)–N(8)	2.172(5)		
N(1)–Co(1)–N(3)	78.2(2)	N(2)–Co(2)–N(8)	118.2(2)
N(1)–Co(1)–N(4)	123.9(2)	N(2)–Co(2)–F	102.0(2)
N(1)–Co(1)–N(5)	108.9(2)	N(6)–Co(2)–N(7)	81.4(2)
N(1)–Co(1)–O(1)	102.1(2)	N(6)–Co(2)–N(8)	82.0(2)
N(3)–Co(1)–N(4)	81.0(2)	N(6)–Co(2)–F	177.4(2)
N(3)–Co(1)–N(5)	83.0(2)	N(7)–Co(2)–N(8)	121.4(2)
N(3)–Co(1)–O(1)	174.6(2)	N(7)–Co(2)–F	100.2(2)
N(4)–Co(1)–N(5)	119.5(2)	N(8)–Co(2)–F	95.4(2)
N(4)–Co(1)–O(1)	94.4(2)	Co(1)–N(1)–N(2)	135.0(3)
N(5)–Co(1)–O(1)	101.9(2)	Co(2)–N(2)–N(1)	134.8(3)
N(2)–Co(2)–N(6)	79.1(2)	O(1)–H(10)–F	163(5)
N(2)–Co(2)–N(7)	113.0(2)	H(10)–O(1)–H(20)	104(5)

Complex **2b** crystallises in space group $P\bar{1}$ with three acetonitrile solvent molecules per formula unit. The molecular structure of the cation is depicted in Fig. 2. It shows two Co atoms bridged by the pyrazolate moiety and with each cobalt centre being co-ordinated by a tren-type co-ordination subunit of the ligand L^2. As in the case of **1b** a fluoride ion has been abstracted from the BF_4^- starting material, however in the present compound **2b** the shorter chain lengths of the ligand side arms do not favour the formation of sufficiently short Co···Co separations suitable to support the small fluoride anion in a bridging position. Consequently the fluoride ligand is bound only to Co(2) and an additional water molecule is incorporated in order to complete the co-ordination sphere around Co(1). The Co-bound oxygen and fluorine atoms are linked by a strong O–H–F bridge [d(O···F) = 2.437 Å, Table 2], while the other H atom of the water molecule forms a hydrogen bond to the N atom of one of the acetonitrile solvent molecules included in the crystal lattice [d(O···N) = 2.957 Å]. It should be noted that the intramolecular hydrogen bond encountered in **2b** is among the shortest O–H–F bridges characterised structurally, which mostly exhibit O···F distances larger than 2.5 Å.[11,12] Each cobalt centre of the dinuclear cation of **2b** is in a slightly distorted trigonal-bipyramidal environment

with the branching N atoms [N(3) and N(6)] and the O and F atoms, respectively, in the axial positions [N(3)–Co(1)–O(1) 174.6(2), N(6)–Co(2)–F 177.4(2)°]. The angles between the bridgehead amine nitrogen atom [N(3) and N(6)], the respective Co atom and the equatorial nitrogen atoms [N(1), N(4), N(5) and N(2), N(7), N(8), respectively] lie in the range 78.2(2) to 83.0(2)°, thus deviating from the ideal co-ordination angle of 90°. This distortion is due to the limited dimensions of each tren-type co-ordination subunit of the dinucleating ligand framework. Analogous co-ordination geometries of the metal centres have been observed for related mononuclear compounds.[11,13]

The distance Co(2)–F [1.932(3) Å] in complex **2b** is significantly shorter than the corresponding ones in **1b** [Co(1)–F and Co(2)–F 2.077(3) Å], as are the bond lengths Co(1)–N(3) and Co(2)–N(6) [2.403(4)/2.350(5) Å in **1b** *vs.* 2.204(4)/2.201(4) Å in **2b**]. This indicates that even for the longer side arms in **1b** the dinuclear framework has to be stretched in order to accommodate the small fluoride ion in a bridging position. However, treatment of a solution of **1b** in acetonitrile with small amounts of water, *i.e.* the conditions used to generate **2b**, did not lead to any observable reaction.

If a sample of the crystalline compound **2b** is kept under dynamic vacuum ($<10^{-2}$ mbar) for prolonged periods of time or heated to above 80 °C a change from greenish grey to purple is observed. This process is reversible, causing the material to turn grey again upon exposure to air. A combined TGA/DSC experiment on **2b** revealed that a series of endothermic events takes place in the temperature range 80–100 °C, which are accompanied by a loss of weight of around 2% (melting or further decomposition processes only occur well above 200 °C). The IR spectrum of the purple material **2c** differs from those of **2b** by the lack of the broad bands attributed to O–H vibrations (see above). Considering the given evidence, we assume that the incorporated water molecule in **2b** is reversibly extruded upon conversion into **2c**. However, no definite information about the constitution of the latter compound is yet available.

The large metal–metal separation imposed by the chelating ligand framework of L^2, which obviously renders the small fluoride ion in complex **2b** unsuited to span both Co atoms, should bring about a distinct size selectivity for secondary anions in this type of complex. Therefore we expected a facile displacement of the FHO(H) unit in **2b** by larger moieties capable of locking into the co-ordination pocket created by the two cobalt centres. Treatment of a solution of **2b** with 1 equivalent of KBr caused a spontaneous colour change of the reaction mixture to deep purple, and large purple crystals of the expected product $[Co_2L^2Br][BPh_4]_2$ **3** formed upon slow diffusion of Et_2O into the acetonitrile solution. For comparison, we independently synthesized **3** starting from HL^2 and $CoBr_2$·dme (dme = 1,2-dimethoxyethane) following the general strategy described for the analogous chloro complex.[9a] The molecular structure of the cation of **3**, which crystallises in space group $P\bar{1}$, is depicted in Fig. 3. It is similar to the crystal structure of the analogous Cl-bridged complex.[9a] Although the comparatively larger bromide ion allows for a slightly longer Co···Co distance (3.935 *vs.* 3.833 Å, Table 3) and a smaller bonding angle at the bridging halide in the present case [Co–X–Co 99.3(1)° for X = Br *vs.* 103.9(1)° for X = Cl], the co-ordination geometries around the cobalt centres do not show any significant difference for the two related compounds [compare *e.g.* N_{ax}–Co–X 167.3(2)/166.2(3) (X = Br) *vs.* 166.2(2)/165.9(2)° (X = Cl)]. As a further point of interest we examined whether the geometrical constraints of the dinucleating ligand L^2, which creates a large cavity between the two juxtaposed cobalt atoms, determines the co-ordination mode of a flexidentate ligand like the azide anion. The latter anion is known to be able to connect two metal centres either as a μ-1,3-N_3 bridge or *via* a single nitrogen atom, *i.e.* in the μ-1,1-N_3 mode.[14,15] While in the absence of a primary bridging ligand the role of the azide is largely left

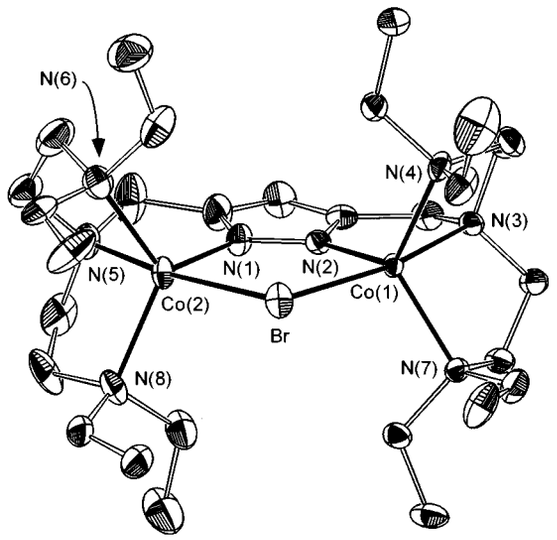

Fig. 3 View of the molecular structure of the cation of complex **3**. Details as in Fig. 1

Table 3 Selected atom distances (Å) and angles (°) for complex **3**

Co(1)–N(2)	1.971(7)	Co(2)–N(5)	2.230(8)
Co(1)–N(3)	2.225(6)	Co(2)–N(6)	2.11(1)
Co(1)–N(4)	2.124(8)	Co(2)–N(8)	2.140(9)
Co(1)–N(7)	2.095(7)	Co(2)–Br	2.601(2)
Co(1)–Br	2.563(2)	N(1)–N(2)	1.34(1)
Co(2)–N(1)	1.981(8)	Co(1)···Co(2)	3.935
N(2)–Co(1)–N(3)	77.8(3)	N(1)–Co(2)–N(8)	114.8(3)
N(2)–Co(1)–N(4)	116.5(3)	N(1)–Co(2)–Br	88.9(2)
N(2)–Co(1)–N(7)	114.1(3)	N(5)–Co(2)–N(6)	82.4(4)
N(2)–Co(1)–Br	89.9(2)	N(5)–Co(2)–N(8)	82.7(3)
N(3)–Co(1)–N(4)	83.2(3)	N(5)–Co(2)–Br	166.2(3)
N(3)–Co(1)–N(7)	82.2(3)	N(6)–Co(2)–N(8)	120.7(4)
N(3)–Co(1)–Br	167.3(2)	N(6)–Co(2)–Br	104.7(2)
N(4)–Co(1)–N(7)	122.3(3)	N(8)–Co(2)–Br	103.1(2)
N(4)–Co(1)–Br	99.9(2)	Co(1)–Br–Co(2)	99.3(1)
N(7)–Co(1)–Br	106.0(2)	Co(1)–N(2)–N(1)	130.6(5)
N(1)–Co(2)–N(5)	77.3(3)	Co(2)–N(1)–N(2)	130.9(5)
N(1)–Co(2)–N(6)	117.1(4)		

to chance, control of the dinuclear centre dimensions and hence control over the azide bridging mode recently gained particular interest with regard to a study of the geometry-dependent magnetic superexchange propagated by the azide bridge.[15,16] In the present case the large metal–metal separation imposed by the ligand framework L^2 was supposed to prevent a μ-1,1-N_3 bridge and to force the azide to adopt the μ-1,3-N_3 mode.

Similar to the above-mentioned replacement of the bridging FHO(H) moiety in complex **2b** by bromide ions, addition of 1 equivalent of NaN_3 to a solution of **2b** in acetonitrile caused a change to deep purple, and crystals of the expected azide-bridged complex $[Co_2L^2(N_3)][BPh_4]_2$ **4** were obtained by slow diffusion of Et_2O into an acetone solution of the product. Complex **4** had been prepared previously by Okawa and co-workers,[6c] however no definite structural information could be obtained. The IR spectrum of **4** shows a strong absorption at 2064 cm^{-1} attributed to the N_3 stretching vibration, this value being similar to the band position previously observed for a μ-1,3-azide in a bridging position between two cobalt centres.[17] The molecular structure of the cation of **4**, which crystallises in the monoclinic space group $P2_1/n$, is depicted in Fig. 4. In accord with the IR data the azide bridge spans the two cobalt centres by the terminal nitrogen atoms N(9) and N(11), thereby stretching the Co···Co distance to 4.415 Å (Table 4). The N_3 moiety is almost linear [N(9)–N(10)–N(11) 176(1)°] with angles Co–N–N of 116.8(6) and 118.4(5)°. The co-ordination geom-

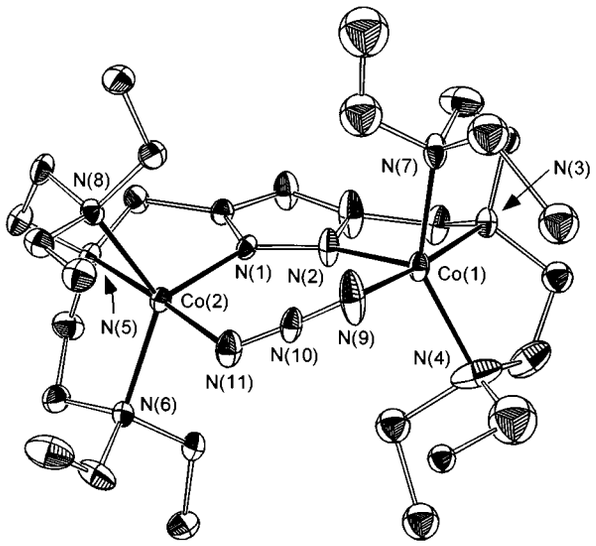

Fig. 4 View of the molecular structure of the cation of complex **4**. Details as in Fig. 1

Table 4 Selected atom distances (Å) and angles (°) for complex **4**

Co(1)–N(2)	2.038(6)	Co(2)–N(6)	2.158(6)
Co(1)–N(3)	2.167(5)	Co(2)–N(8)	2.162(6)
Co(1)–N(4)	2.089(8)	Co(2)–N(11)	2.062(7)
Co(1)–N(7)	2.07(1)	N(1)–N(2)	1.384(8)
Co(1)–N(9)	2.074(8)	N(9)–N(10)	1.15(1)
Co(2)–N(1)	2.043(5)	N(10)–N(11)	1.139(9)
Co(2)–N(5)	2.177(6)	Co(1)···Co(2)	4.415
N(2)–Co(1)–N(3)	80.9(2)	N(1)–Co(2)–N(11)	99.5(3)
N(2)–Co(1)–N(4)	109.4(4)	N(5)–Co(2)–N(6)	82.0(2)
N(2)–Co(1)–N(7)	100.1(4)	N(5)–Co(2)–N(8)	82.7(2)
N(2)–Co(1)–N(9)	98.5(3)	N(5)–Co(2)–N(11)	175.8(3)
N(3)–Co(1)–N(4)	82.5(3)	N(6)–Co(2)–N(8)	128.9(2)
N(3)–Co(1)–N(7)	83.0(3)	N(6)–Co(2)–N(11)	94.4(3)
N(3)–Co(1)–N(9)	174.8(4)	N(8)–Co(2)–N(11)	101.3(3)
N(4)–Co(1)–N(7)	144.4(5)	Co(1)–N(2)–N(1)	138.0(4)
N(4)–Co(1)–N(9)	102.5(4)	Co(2)–N(1)–N(2)	136.2(4)
N(7)–Co(1)–N(9)	92.1(5)	Co(1)–N(9)–N(10)	116.8(6)
N(1)–Co(2)–N(5)	80.0(2)	Co(2)–N(11)–N(10)	118.4(5)
N(1)–Co(2)–N(6)	113.2(2)	N(9)–N(10)–N(11)	176(1)
N(1)–Co(2)–N(8)	111.6(2)		

etry around the cobalt centres is similar to those in the starting material **2b**, *i.e.* distorted trigonal bipyramidal with the branching nitrogen atoms of the side arms of L^2 [N(3) and N(5)] and the co-ordinating outer nitrogen atoms of the secondary azide ligand [N(9) and N(11)] in the axial positions. The two cobalt atoms are 0.33 Å above and below the plane defined by the pyrazolate heterocycle, respectively. With the middle N atom of the azide being situated roughly within this plane (distance 0.07 Å), the bond axis N(9)–N(10)–N(11) intersects the plane defined by the pyrazolate by an angle of around 25°.

Thus the framework of linked tren-type co-ordination subunits in the pyrazolate-based dinuclear complexes described here proves flexible enough to adapt to various secondary bridges of sufficiently large size, while small monoatomic bridges can be prevented by the use of appropriate short side arms. Thereby the co-ordination geometry around the metal ions remains within the variable types of five-co-ordination, *i.e.* between square pyramidal and trigonal bipyramidal. Five-co-ordination of the cobalt(II) centres in solution is corroborated by the UV/VIS spectra for all complexes studied (Table 5).[18]

Magnetic properties of complexes 3 and 4

The magnetic properties of complexes **3** and **4** were studied over the temperature range 8–290 K. Magnetic susceptibility data

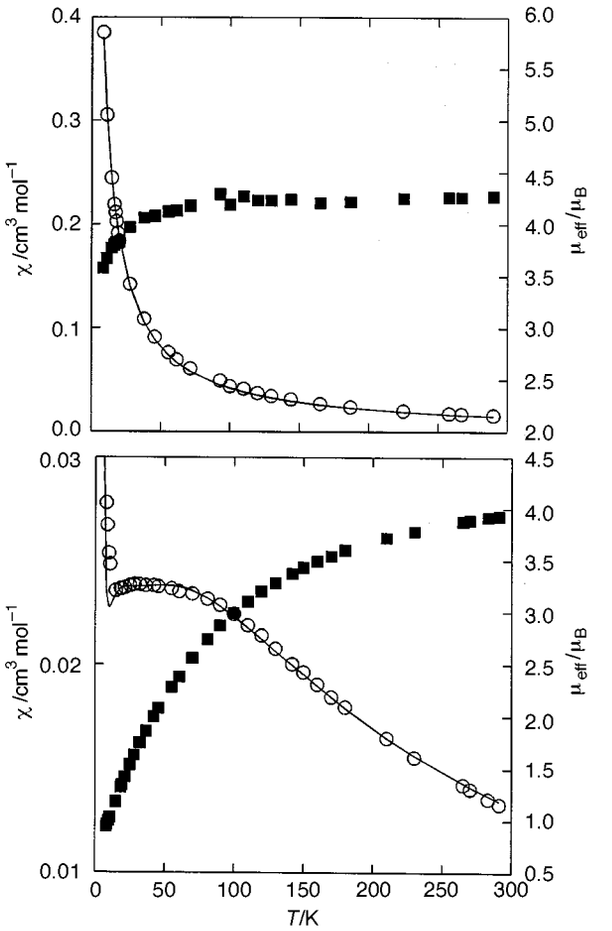

Fig. 5 Temperature dependence of the magnetic susceptibility (open circles) and magnetic moment (solid squares) per cobalt atom for complexes **3** (top) and **4** (bottom). The line represents the calculated curve

Table 5 The UV/VIS data of the complexes ($\tilde{\nu}$/cm^{-1}, ε/M^{-1} cm^{-1})

Complex	
1a	12 030 (40), 17 670 (sh, 150), 18 730 (195), 19 420 (sh, 190)
1b	12 350 (67), 18 350 (200), 19 450 (190)
2a	14 180 (30), 18 180 (85), 20 490 (115)
2b	13 300 (54), 16 750 (66), 20 600 (210)
3	13 190 (47), 17 920 (153), 19 530 (sh, 158), 20 000 (160)
4	13 700 (54), 16 860 (180), 19 530 (140)

for the Br-bridged compound reveal Curie–Weiss law behaviour over a wide temperature range (linear regression yields $C = 4.61$, $\theta = -4.30$ K) with a magnetic moment of 4.29 ± 0.04 μ_B per cobalt atom, this value being significantly higher than the spin-only value for a high spin $S = \frac{3}{2}$ situation (3.87 μ_B). The observed value corresponds well to those generally reported for mononuclear trigonal-bipyramidal high spin cobalt(II) complexes with a N_4Br donor set, which were shown to exhibit magnetic moments in the range 4.1–4.8 μ_B.[19] Fitting the experimental data by the theoretical expression of the isotropic Heisenberg model ($H = -2JS_1S_2$) for the $S_1 = S_2 = \frac{3}{2}$ spin-only situation[20] confirms a very weak antiferromagnetic coupling of $-1 < J < 0$ cm^{-1}.

In contrast to a previous report,[6c] we find that the variable-temperature molar susceptibility for complex **4** (Fig. 5) goes through a broad maximum at around 30 K, indicative of antiferromagnetic coupling between the two cobalt centres. A rise of the susceptibility at very low temperatures is probably due to the presence of small amounts of uncoupled paramagnetic impurity. The effective magnetic moment per cobalt ion decreases from 3.93 μ_B at 290 K to 0.94 μ_B at 8 K. Such a

behaviour is indeed expected, as the superexchange propagated by the μ-1,3-bridging mode of azide is assumed to be exclusively antiferromagnetic in nature.[16] Attempts were made to fit the susceptibility data for **4** by the theoretical expression of the isotropic for the $S_1 = S_2 = \frac{3}{2}$ spin only situation,[20] however an acceptable fit (with $J = -12.0$ cm^{-1}) could only be obtained with an unreasonably low g value of 1.83. The inability satisfactorily to model the experimental data presumably arises from the neglect of unquenched orbital angular momentum and zero-field-splitting effects, which should be included for a more detailed analysis of the magnetic behaviour of **4**.[21]

Conclusion

The present work shows that the accessible range of metal–metal separations in bimetallic pyrazolate-based entities can effectively be tuned by different chelating side arms in the 3 and 5 positions of the heterocycle. Dinuclear cobalt(II) complexes of both L^1 (having more flexible C_3 links between the side arm donor atoms) and L^2 (with shorter C_2 units within the substituents) readily abstract a fluoride from BF_4^- counter anions. However, while in **1b** the fluoride occupies a bridging position between the two cobalt centres that are held at a distance of 3.577 Å, the shorter chelating side arms of L^2 pull the metal ions back and apart, thus preventing small moieties like fluoride from spanning both metal centres in a bridging fashion. In the present case **2b** an additional water molecule is thus incorporated, forming a short intramolecular F–H–O(H) bond between the two cobalt atoms that are located at a distance of 4.282 Å. Evidence from IR and TGA/DSC measurements suggests that the water molecule can be reversibly extruded under vacuum or at elevated temperatures. Compound **2b** serves as a suitable starting material for the introduction of various secondary bridges into pyrazolate-based dinuclear complexes *via* substitution of the labile FHO(H) group. This is illustrated by treating **2b** with KBr or NaN_3, thereby generating the bromide- and azide-bridged species **3** and **4**, respectively. In the latter compound the large metal–metal separation imposed by the primary ligand framework L^2 forces the azide to adopt a μ-1,3 bridging mode. As expected and in contrast to a previous report,[6c] this mode propagates antiferromagnetic coupling between the two high-spin d^7 cobalt(II) centres, which underlines the importance of designed dinuclear systems in the quest to influence co-operative magnetic properties in a controlled fashion. Furthermore the adjustment of the metal–metal separation in this type of dinuclear complex should allow for the tuning of possible co-operative reactivity at the bimetallic core, *e.g.* the generation of a highly nucleophilic metal-bonded hydroxide (similar in size to fluoride) that is prevented from spanning both metal centres and thus might develop its nucleophilicity towards various substrate molecules. Work in this regard is presently in progress.

Experimental

All manipulations were carried out under an atmosphere of dry nitrogen by employing standard Schlenk techniques. Solvents were dried according to established procedures. The compounds HL^1 and HL^2 were synthesized according to the reported method.[9a] Microanalyses: Mikroanalytische Laboratorien des Organisch-Chemischen Instituts der Universität Heidelberg. IR spectra: Bruker IFS 66 FTIR. FAB and EI mass spectra: Finnigan MAT 8230. UV/VIS/NIR spectra: Perkin-Elmer Lambda 19. Magnetic measurements: Bruker B-E 15 C8 magnet, B-H 15 field controller, ER4111VT variable-temperature unit, Sartorius M 25 D-S micro balance. TGA/DSC: Mettler system TA 4000, TC 11 processor and TG 50 thermobalance.

Preparations

Complexes 1a and 1b. A solution of HL^1 (0.25 g, 0.54 mmol) in tetrahydrofuran (thf, 25 cm^3) was treated with 1 equivalent of LiBu (2.5 M in hexane) and stirred for 15 min at room temperature. All volatile material was removed under vacuum and the residue was taken up in MeCN (25 cm^3). Anhydrous $[Co(MeCN)_6][BF_4]_2$ (0.52 g, 1.08 mmol) was added in one portion, the now purple reaction mixture being kept stirred for 15 min and finally $NaBPh_4$ (0.37 g, 1.08 mmol) was added. After stirring for 15 min the volume of the solution was reduced to ≈5 cm^3 and Et_2O (40 cm^3) added, causing the formation of a purple precipitate. This was filtered off, washed twice with Et_2O and dried under vacuum to yield 0.55 g (0.42 mmol, 78%). $[Co_2L^1(BF_4)][BPh_4]_2$ **1a** (Found: C, 67.14; H, 7.51; N, 8.56. $C_{73}H_{93}B_3Co_2F_4N_8$ requires C, 66.99; H, 7.16; N, 8.56%); $\tilde{\nu}$/cm^{-1} 3052m, 2979m, 1948w, 1881w, 1828w, 1635m, 1614m, 1579s, 1479s, 1065s (br), 802s, 747s, 734s, 705s and 612m. Vapour diffusion of Et_2O into a solution of **1a** in MeCN afforded purple crystals of $[Co_2L^1F][BPh_4]_2$ **1b** (0.30 g, 0.37 mmol) (Found: C, 70.40; H, 7.84; N, 9.18. $C_{73}H_{93}B_2Co_2FN_8$ requires C, 70.65; H, 7.55; N, 9.03%); $\tilde{\nu}$/cm^{-1} 3053m, 2978m, 1948, 1881, 1822w, 1579m, 1478s, 748s, 735s, 707s and 612s.

Complexes 2a and 2b. A solution of HL^2 (0.28 g, 0.54 mmol) in thf (25 cm^3) was treated with 1 equivalent of LiBu (2.5 M in hexane) and stirred for 15 min at room temperature. All volatile material was then removed under vacuum and the residue taken up in MeCN (25 cm^3). Anhydrous $[Co(MeCN)_6][BF_4]_2$ (0.52 g, 1.08 mmol) was added in one portion, the now purple reaction mixture being kept stirred for 15 min and finally $NaBPh_4$ (0.37 g, 1.08 mmol) was added. After stirring for 15 min the volume of the solution was reduced to ≈5 cm^3 and Et_2O (40 cm^3) added, causing the formation of a light violet precipitate. This was filtered off, washed twice with Et_2O and dried under vacuum to yield 0.64 g (0.47 mmol, 87%) $[Co_2L^2(BF_4)][BPh_4]_2$ **2a** (Found: C, 67.58; H, 7.89; N, 8.65. $C_{77}H_{101}B_3Co_2F_4N_8$ requires C, 67.75; H, 7.46; N, 8.21%); $\tilde{\nu}$/cm^{-1} 3055m, 2983m, 1941w, 1888w, 1828w, 1579m, 1478s, 1077s (br), 735s, 707s and 610s. Treatment of a solution of **2a** in MeCN (8 cm^3) with water (0.1 cm^3), followed by EtOH (20 cm^3), caused decolorisation and precipitation of a pale grey solid which was filtered off and dried. Vapour diffusion of Et_2O into a solution of this material in wet MeCN afforded greenish grey crystals of $[Co_2L^2(F)(H_2O)][BPh_4]_2\cdot 3MeCN$ **2b**·3MeCN (0.46 g, 0.32 mmol) (Found: C, 69.19; H, 8.12; N, 10.70. $C_{77}H_{103}B_2Co_2FN_8O\cdot C_6H_9N_3$ requires C, 69.31; H, 7.85; N, 10.71%); $\tilde{\nu}$/cm^{-1} 3471m (br), 3055m, 2981m, 2612m (br), 2251m, 1941, 1888, 1828w, 1579m, 1477s, 735s, 707s and 610s; *m*/*z* 735 {100, $[L^2Co_2F(Ph)]^+$} and 677 {52%, $[L^2Co_2F(H_2O) + 1]^+$}.

Complex 3. A solution of complex **2b** (0.40 g, 0.30 mmol) in MeCN (20 cm^3) was treated with KBr (0.04 g, 0.34 mmol) and stirred for 30 min at room temperature, causing the reaction mixture to turn purple. All volatile material was then evaporated in vacuum, the residue taken up in MeCN (20 cm^3) and filtered. Vapour diffusion of Et_2O into the MeCN solution afforded purple crystals of $[Co_2L^2Br][BPh_4]_2\cdot 0.25\ Et_2O\cdot 1.38$ MeCN **3**·0.25 Et_2O·1.38 MeCN; (0.27 g, 0.19 mmol, 63%) (Found: C, 67.81; H, 7.58; N, 8.36. $C_{77}H_{101}B_2BrCo_2N_8$ requires C, 68.10; H, 7.50; N, 8.25%); $\tilde{\nu}$/cm^{-1} 3054m, 2981m, 1941w, 1881w, 1820w, 1579m, 1478s, 735s, 705s and 611s. Complex **3** can alternatively be prepared from HL^2 and $CoBr_2\cdot$dme following a procedure described previously for $[Co_2L^2(Cl)][BPh_4]_2$.[9a]

Complex 4. A solution of complex **2b** (0.40 g, 0.30 mmol) in MeCN (20 cm^3) was treated with NaN_3 (0.02 g, 0.31 mmol) and stirred for 30 min at room temperature, causing the reaction mixture to turn purple. All volatile material was then evaporated in vacuum, the residue taken up in acetone (20 cm^3) and filtered. Layering the acetone solution with light petroleum (b.p. 40–60 °C) afforded purple crystals of $[Co_2L^2(N_3)][BPh_4]_2\cdot Me_2CO$ **4**·Me_2CO (0.30 g, 0.21 mmol, 70%) (Found: C, 69.58; H, 8.00; N, 10.71. $C_{77}H_{101}B_2Co_2N_{11}\cdot C_6H_3O$ requires C, 69.72; H,

Table 6 Crystal data and refinement details for complexes **1b**, **2b**, **3** and **4**

	1b	**2b**	**3**	**4**
Formula	$C_{73}H_{93}B_2Co_2FN_8$	$C_{77}H_{103}B_2Co_2FN_8O\cdot 3\,C_2H_3N$	$C_{77}H_{101}B_2BrCo_2N_8\cdot 0.25\,C_2H_{10}O\cdot 1.38\,C_2H_3N$	$C_{77}H_{101}B_2Co_2N_{11}\cdot C_3H_6O$
M_r	1241.08	1438.3	1433.0	1378.3
Crystal size/mm	0.30 × 0.30 × 0.30	0.85 × 0.50 × 0.20	0.30 × 0.35 × 0.30	0.25 × 0.25 × 0.15
Crystal system	Triclinic	Triclinic	Triclinic	Monoclinic
Space group	$P\bar{1}$	$P\bar{1}$	$P\bar{1}$	$P2_1/n$
a/Å	11.774(1)	12.445(6)	12.822(2)	12.372(2)
b/Å	14.606(2)	13.038(8)	15.234(3)	21.443(6)
c/Å	19.919(3)	24.61(1)	23.070(3)	29.265(5)
α/°	100.02(1)	90.43(5)	72.44(1)	—
β/°	99.47(1)	96.31(4)	74.34(1)	94.65(1)
γ/°	101.16(1)	91.15(5)	66.65(1)	—
U/Å^3	3239(1)	3968(4)	3886(1)	7738(3)
D_c/g cm^{-3}	1.272	1.204	1.225	1.154
Z	2	2	2	4
F(000)	1320	1536	1517	2808
T/K	200	203	200	200
μ(Mo-Kα)/mm^{-1}	0.564	0.472	0.989	0.478
Scan mode	ω	ω	ω	ω
hkl Ranges	0–13, ±16, ±23	±15, ±16, 0–30	0–15, −16 to 17, −26 to 27	−14–0, 0–20, ±34
2θ Range/°	4.1–50.0	3.1–52.0	3.0–50.1	3.4–50.0
Measured reflections	11 941	16 974	14 385	12 521
Observed reflections [$I > 2\sigma(I)$]	6335	7787	6933	7954
Refined parameters	786	926	888	879
Residual electron density/e Å^{-3}	0.697, −0.760	0.532, −0.402	1.042, –1.185	1.386, −0.664
$R1$	0.072	0.068	0.099	0.096
$wR2$ (refinement on F^2)	0.177	0.169	0.304	0.293
Goodness of fit	1.015	1.006	1.177	1.049

7.82; N, 11.18%); ν̃/cm^{-1} 3053m, 2985m, 2064s, 1950w, 1881w, 1817w, 1710s, 1579m, 1474s, 735s, 706s and 611s; *m*/*z* 1000 {26, $[L^2Co_2(N_3)(BPh_4)]^+$}, 758 {100, $[L^2Co_2(N_3)Ph]^+$} and 683 {50%, $[L^2Co_2(N_3) + 1]^+$}.

Crystallography

The measurements were carried out on a Siemens P4 (Nicolet Syntex) R3m/v (complexes **1b**, **3** and **4**) or on a Siemens-Stoe AED2 (**2b**) four-circle diffractometer with graphite-monochromated Mo-Kα radiation (λ 0.710 73 Å). All calculations were performed with a micro-vax computer using the SHELXTL PLUS software package.[22] Structures were solved by direct methods with the SHELXS 86 and refined with the SHELXL 93 programs.[22] An absorption correction (ψ scan, $\Delta\psi = 10°$) was applied to all data. Atomic coordinates and anisotropic thermal parameters of the non-hydrogen atoms were refined by full-matrix least-squares calculation. The hydrogen atoms were placed at calculated positions, except for the bridging hydrogen atoms H(10) and H(20) in **2b** which were located in the difference Fourier map and refined. Owing to the moderate quality of the crystals and disorder problems the structure analyses of **3** and **4** could only be refined to final (poor) agreement values of $R = 0.099$ and 0.096, respectively. In the case of **3** the solvent molecules included in the crystal lattice showed disorder and were thus only refined isotropically. In the case of **4** the acetone solvent molecule was located at two different positions and the side arm atoms around Co(1) were severely disordered and in part only refined isotropically. Table 6 compiles the data for the structure determinations.

CCDC reference number 186/781.

See http://www.rsc.org/suppdata/dt/1998/207/ for crystallographic files in .cif format.

Acknowledgements

We are grateful to Professor Dr. G. Huttner for his generous and continuous support of our work as well as to the Deutsche Forschungsgemeinschaft (Habilitandenstipendium for F. M.) and the Fonds der Chemischen Industrie.

References

1 K. D. Karlin, *Science*, 1993, **261**, 701; J. Reedijk, *Bioinorganic Catalysis*, Marcel Dekker, New York, 1993; R. H. Holm, *Pure Appl. Chem.*, 1995, **67**, 217; H. Steinhagen and G. Helmchen, *Angew. Chem., Int. Ed. Engl.*, 1996, **35**, 2339; N. Sträter, W. N. Lipscomb, T. Klabunde and B. Krebs, *Angew. Chem., Int. Ed. Engl.*, 1996, **35**, 2024.

2 See, for example, S. R. Collinson and D. E. Fenton, *Coord. Chem. Rev.*, 1996, **148**, 19; H. Okawa and H. Sakiyama, *Pure Appl. Chem.*, 1995, **67**, 273; L. Que, jun. and Y. Dong, *Acc. Chem. Res.*, 1996, **29**, 190; D. E. Fenton and H. Okawa, *Chem. Ber./Recueil*, 1997, **130**, 433.

3 See, for example, R. Robson, *Inorg. Nucl. Chem. Lett.*, 1970, **6**, 125; K. D. Karlin, J. C. Hayes, Y. Gultneh, R. W. Cruse, J. W. McKnown, J. P. Hutchinson and J. Zubieta, *J. Am. Chem. Soc.*, 1984, **106**, 2121; T. N. Sorrell, D. L. Jameson and C. J. O'Connor, *Inorg. Chem.*, 1984, **23**, 190; Y. Nishida, H. Shimo, H. Maehara and S. Kida, *J. Chem. Soc., Dalton Trans.*, 1985, 1945; D. Volkmer, B. Hommerich, K. Griesar, W. Haase and B. Krebs, *Inorg. Chem.*, 1996, **35**, 3792.

4 P. J. Steel, *Coord. Chem. Rev.*, 1990, **106**, 227; A. P. Sadimenko and S. S. Basson, *Coord. Chem. Rev.*, 1996, **147**, 247.

5 T. G. Schenck, J. M. Downes, C. R. C. Milne, P. B. Mackenzie, H. Boucher, J. Whelan and B. Bosnich, *Inorg. Chem.*, 1985, **24**, 2334.

6 (*a*) T. Kamiusuki, H. Okawa, E. Kitaura, M. Koikawa, N. Matsumoto, S. Kida and H. Oshio, *J. Chem. Soc., Dalton Trans.*, 1989, 2077; (*b*) T. Kamiusuki, H. Okawa, N. Matsumoto and S. Kida, *J. Chem. Soc., Dalton Trans.*, 1990, 195; (*c*) T. Kamiusuki, H. Okawa, E. Kitaura, K. Inoue and S. Kida, *Inorg. Chim. Acta*, 1991, **179**, 139; (*d*) M. Itoh, K. Motoda, K. Shindo, T. Kamiusuki, H. Sakiyama, N. Matsumoto and H. Okawa, *J. Chem. Soc., Dalton Trans.*, 1995, 3635.

7 B. Mernari, F. Abraham, M. Lagrenee, M. Drillon and P. Legoll, *J. Chem. Soc., Dalton Trans.*, 1993, 1707.

8 L. Behle, M. Neuburger, M. Zehnder and T. A. Kaden, *Helv. Chim. Acta*, 1995, **78**, 693.

9 (*a*) F. Meyer, S. Beyreuther, K. Heinze and L. Zsolnai, *Chem. Ber./Recueil*, 1997, **130**, 605; (*b*) F. Meyer, A. Jacobi and L. Zsolnai, *Chem. Ber./Recueil*, 1997, **130**, 1441.

10 T. R. Musgrave and T. S. Lin, *J. Coord. Chem.*, 1973, **2**, 323; M. A. Guichelaar, J. A. M. van Hest and J. Reedijk, *Inorg. Nucl. Chem. Lett.*, 1974, **10**, 999; F. J. Rietmeyer, R. A. G. de Graaf and J. Reedijk, *Inorg. Chem.*, 1984, **23**, 151; S. C. Lee and R. H. Holm, *Inorg. Chem.*, 1993, **32**, 4745.

11 G. J. van Driel, W. L. Driessen and J. Reedijk, *Inorg. Chem.*, 1985, **24**, 2919.
12 P. Bukovec, S. Milicev, A. Demšar and L. Golic, *J. Chem. Soc.*, *Dalton Trans.*, 1981, 1802; A. J. Blake, M. A. Halcrow and M. Schröder, *J. Chem. Soc.*, *Dalton Trans.*, 1992, 2803; P. J. van Koningsbruggen, J. G. Haasnot, R. A. G. de Graaf and J. Reedijk, *J. Chem. Soc.*, *Dalton Trans.*, 1993, 483.
13 A. M. Dittler-Klingemann and F. E. Hahn, *Inorg. Chem.*, 1996, **35**, 1996; C. Benelli, I. Bertini, M. Di Vaira and F. Mani, *Inorg. Chem.*, 1984, **23**, 1422.
14 Z. Dori and R. F. Ziolo, *Chem. Rev.*, 1973, **73**, 247.
15 J. Ribas, M. Montfort, B. K. Gosh and X. Solans, *Angew. Chem.*, *Int. Ed. Engl.*, 1994, **33**, 2087; J. Ribas, M. Montfort, B. K. Gosh, R. Cortes, X. Solans and M. Font-Bardia, *Inorg. Chem.*, 1996, **35**, 864.
16 O. Kahn, in *Magneto Structural Correlations in Exchange Coupled Systems*, eds. R. D. Willet, D. Gatteschi and O. Kahn, Reidel, Dordrecht, 1985, p. 57; L. K. Thompson and S. S. Tandon, *Comments Inorg. Chem.*, 1996, **18**, 125.
17 A. Bencini, C. A. Ghilardi, S. Midollini and A. Orlandini, *Inorg. Chem.*, 1989, **28**, 1958.
18 M. Ciampolini, N. Nardi and G. P. Speroni, *Coord. Chem. Rev.*, 1966, **1**, 222; C. Furlani, *Coord. Chem. Rev.*, 1968, **3**, 141.
19 M. Ciampolini and N. Nardi, *Inorg. Chem.*, 1966, **5**, 41; L. V. Interrante and J. L. Shafer, *Inorg. Nucl. Chem. Lett.*, 1968, **4**, 411; A. Dei and R. Morassi, *J. Chem. Soc. A*, 1971, 2024; L. K. Thompson, B. S. Ramaswamy and E. A. Seymour, *Can. J. Chem.*, 1977, **55**, 878.
20 C. J. O'Connor, *Prog. Inorg. Chem.*, 1982, **29**, 203.
21 M. E. Lines, *J. Chem. Phys.*, 1971, **55**, 2977.
22 G. M. Sheldrick, SHELXTL PLUS, Program Package for Structure Solution and Refinement, Siemens Analytical Instruments, Madison, WI, 1990; SHELXL 93, Program for Crystal Structure Refinement, Universität Göttingen, 1993; G. M. Sheldrick, SHELXS-86, Program for Crystal Structure Solution, Universität Göttingen, 1986.

Received 31*st July* 1997; *Paper* 7/05545E